Pharm Res (2011) 28:1520–1530
DOI 10.1007/s11095-011-0453-2

RESEARCH PAPER

Agarose Surface Coating Influences Intracellular Accumulation and Enhances Payload Stability of a Nano-delivery System

Enrica De Rosa • Ciro Chiappini • Dongmei Fan • Xuewu Liu • Mauro Ferrari • Ennio Tasciotti

Received: 31 December 2010 / Accepted: 15 April 2011 / Published online: 24 May 2011

ABSTRACT

Purpose Protein therapeutics often require repeated administrations of drug over a long period of time. Protein instability is a major obstacle to the development of systems for their controlled and sustained release. We describe a surface modification of nanoporous silicon particles (NSP) with an agarose hydrogel matrix that enhances their ability to load and release proteins, influencing intracellular delivery and preserving molecular stability.

Methods We developed and characterized an agarose surface modification of NSP. Stability of the released protein after enzymatic treatment of loaded particles was evaluated with SDS-page and HPLC analysis. FITC-conjugated BSA was chosen as probe protein and intracellular delivery evaluated by fluorescence microscopy.

Results We showed that agarose coating does not affect NSP protein release rate, while fewer digestion products were found in the released solution after all the enzymatic treatments. Confocal images show that the hydrogel coating improves intracellular delivery, specifically within the nucleus, without affecting the internalization process.

Conclusions This modification of porous silicon adds to its tunability, biocompatibility, and biodegradability the ability to preserve protein integrity during delivery without affecting release rates and internalization dynamics. Moreover, it may allow the silicon particles to function as protein carriers that enable control of cell function.

KEY WORDS agarose hydrogel · intracellular delivery · nanopores · porous silicon · protein

ABBREVIATIONS

A1	agarose composition 0.125%
A2	agarose composition 0.05%
Ag	agarose coated
APTES	aminopropyltriethoxysilane
BSA	bovine serum albumin
FACS	fluorescence activated cell sorting
FGF	fibroblast growth factor
HPLC	high performance liquid chromatography
HUVEC	human umbilical vein endothelial cells
NC	bare / not coated
NSPs	nanoporous silicon particles
PLGA	poly(lactic-co-glycolic acid)
pSi	porous silicon
SDS-page	sodium dodecyl sulfate polyacrylamide gel electrophoresis
SEM	scanning electron microscope
SiN	silicon nitride
VEGF	vascular endothelial growth factor

INTRODUCTION

During the last few decades, protein therapeutics have developed dramatically and gained a significant role in many fields of medicine (1). Proteins such as growth factors,

Electronic Supplementary Material The online version of this article (doi:10.1007/s11095-011-0453-2) contains supplementary material, which is available to authorized users.

E. De Rosa • D. Fan • X. Liu • M. Ferrari • E. Tasciotti (✉)
The Methodist Hospital Research Institute (TMHRI)
6670 Bertner Av# Suite R7-114
Houston, Texas 77030, USA
e-mail: etasciotti@tmhs.org

C. Chiappini
University of Texas at Austin
10100 Burnet Rd, Bld. 160
Austin, Texas 78758, USA

hormones, and cytokines are achieving widespread recognition as therapeutic agents (2), while protein epitopes are now being mapped and used for vaccination that provides broad protection against infectious agents (3). Various therapeutic proteins have been proposed in the literature with a wide range of roles and functions in the body (4–7): formation of receptor domains on the cell surface, improvement of the intracellular and/or extracellular molecular transport, enzymatic catalysis of biochemical reactions, enzymatic or regulatory activity, targeting, vaccines (8,9), and diagnostics (10–12). Protein drugs are able to act selectively on biological pathways but often require repeated administration, making their clinical use even more challenging than that of conventional drugs (13–16). The controlled and sustained release of proteins may enhance their therapeutic efficacy and reduce the pain and inconvenience of frequent injections. However, intravenous administration faces a single major issue: protein instability (17). Structurally unstable proteins are rapidly degraded and deactivated by specific enzymes upon systemic injection (18). Growth factors such as FGF and VEGF, for example, have half-lives as short as 3 and 50 min, respectively (19,20). Furthermore, sustained release (days to months) and formulation of the delivery system often exposes proteins to harmful agents that may disrupt their integrity and ultimately compromise their therapeutic efficacy (21,22).

In the past few years, many drug delivery systems have been developed. Some organic ones (e.g. liposomes, micelles, nanoparticles) are able to deliver drugs to a specific site and at the desired rate, yet most of these systems are rapidly eliminated by the reticulum endothelial system (RES). Furthermore, polymeric formulations (such as PLGA), release acidic byproducts upon degradation and can induce local inflammatory responses that negatively impact protein integrity and activity (23,24).

Porous silicon (pSi) has been proposed as an ideal biomaterial for drug delivery thanks to its biocompatibility (25,26), tunability of the porous structure (27,28), ease and versatility of processing through standard semiconductor technology (29,30), and the well-established protocols for the optimization of its surface chemistry (31,32). As a result, pSi has been successfully used to improve drug solubility, increase bioavailability, and modulate release rates, thus paving a promising path for the realization of pSi drug delivery devices (33–35). pSi has been successfully employed for the loading and release of peptides, proteins, and nanoparticles in a controlled and sustained fashion (35–38). Peptides loaded into porous silicon particles have been systemically delivered *in vivo*, resulting in a prolonged effect compared to their free administration (39). Post-synthesis modification of pSi provided controlled release and enhanced loading of bioactive molecules (33,36,37,40). However, the stability of the loaded/encapsulated protein has not been guaranteed thus far.

This work describes a novel surface modification with agarose hydrogel developed to enhance protein stability within nanoporous silicon particles (NSP) during sustained and controlled release and during enzymatic digestion. Moreover, we report the coating's control over NSP intracellular trafficking and uptake. The enhancement to protein delivery of this NSP surface matrix coating may extend the use of pSi as a versatile delivery system for enzymes, vaccine antigens, and protein therapeutics in general. In particular, we envision two possible routes of administration of the agarose-coated silicon particles: intravenous injection, already largely and successfully tested *in vivo* (41–43), or surgical implantation as a component of a scaffold for tissue engineering applications. Finally, subcutaneous delivery of these particles might be envisioned, although it has not been tested so far.

MATERIALS AND METHODS

Nanoporous Silicon Particles Synthesis and APTES Modification

NSPs were designed and fabricated in the Microelectronics Research Center at the University of Texas at Austin by established methods (29,35). In brief, after low pressure chemical vapor deposition of 100 nm silicon nitride (SiN), photoresist was spun cast on a 100 mm, 0.005 Ω-cm p-type Si wafer. A pattern consisting of 2 μm dark field circles with 2 μm pitch was transferred to the photoresist by contact photolitography. Then the pattern was transferred for 100 nm into the silicon substrate by reactive ion etching with CF_4 gas. The photoresist was removed from the substrate for anodic etch preparation by piranha clean. The porous particles were formed by selective porosification through the SiN mask by anodic etch. The SiN layer was removed by soaking in HF, the substrate was dried, and the particles were released in isopropanol by sonication. Particles were then oxidized by piranha (solution of 2:1 vol. H2SO4 (96%) in H2O2 (30%)) for 2 h at 120°C, then modified with aminopropyltriethoxysilane ((APTES) 2% in IPA) for 2 h at 35°C to provide a controlled positive charge to the particle surface that enhances protein loading capacity.

Modification of Nanoporous Silicon Particles with Agarose Matrix

Agarose coating was performed by suspending NSPs in warm (40°C) agarose solution for 15 min, and then the solution was cooled at 4°C for 30 min. Agarose coating

solutions were prepared at different concentrations ranging from 0.05 to 0.5%$_w$ with low melt certified agarose (BIORAD), used as received. To remove excess gel, particles were washed with warm PBS (35°C) and cooled at room temperature twice. Agarose coating of loaded NSPs was performed after loading before any washing step.

NSP Characterization

The volume, size, and concentration of NSPs were characterized by a MultisizerTM 4 Coulter Counter (Beckman Coulter). Before the analysis, the samples were dispersed in the balanced electrolyte solution (ISOTON VR II Diluent, Beckman Coulter Fullerton, CA) and sonicated for 5 s to ensure a homogenous dispersion. Their surface charge before and after APTES modification and agarose coating was measured in a PB buffer at pH 7.4 using a ZetaPALS Zeta Potential Analyzer (Brookhaven Instruments Corporation; Holtsville, NY). The surface area and pore size distribution of the NSPs were measured using N2 adsorption-desorption isotherms on a Quantachrome Autosorb-3B Surface Analyzer. To prepare the sample, 10 mg of NSPs were transferred to a sample cell and dried in a vacuum oven at 80°C. The sample was degassed at 200°C for 12 h, and the N2 adsorption-desorption isotherm was measured at 77 K over the relative pressure (P/P0) range of 0.015–0.995. Nanopore size distributions and porosities were calculated from the desorption branch of the isotherms using the BJH model. NSP size and shape were also evaluated at different timepoints during incubation in PBS at room temperature by scanning electron microscope (SEM) (FEI Quanta 400 ESEM FEG). To prepare SEM sample, a drop of PSN IPA solution is directly placed on a clean aluminum SEM sample stub and dried. Ag samples were sputter-coated with gold for 2 min at 10 nm layer using a CrC-150 Sputtering System (Torr International, New Windsor, NY). All the samples were loaded in SEM chamber, and SEM images were measured at 5 kV and 3–5 mm working distance using an In-lens detector. Size variation over time was also examined by fluorescence activated cell sorting (FACS) (Becton Dickinson, FACSCalibur). Solution pH was measured with pH strips (colorPHast – EMD).

Protein Loading and Release

Lyophilized and fluorescein isothiocyanate (FITC)-conjugated bovine serum albumin (BSA) was chosen as a protein probe, purchased from Sigma-Aldrich, and used as received. BSA was loaded into NSPs by suspending 10^8 NSPs in 200 μL of 25 mg/mL BSA (1.2% of BSA was FITC-conjugated) aqueous solution (prepared in PBS—GIBCO Invitrogen). The suspension was continuously mixed in dark at 4°C for 2 h, then spun down, and the supernatant was removed. To remove excess of probe, three washing steps were performed. Coated and not-coated particles underwent the same number of washing steps.

To measure the loading efficiency of NSPs, the fluorescence and concentration of the BSA solution used for the loading (as prepared for the loading procedure and as recovered after incubation) was quantified by spectrofluorimetry with SpectraMax M2 spectrophotometer (Molecular Devices). The BSA loss during coating procedure was also taken into account by measuring coating and washing solutions fluorescence/concentration.

Protein release over time from NSP (bare / not-coated (NC)) and agarose-coated (Ag) with two agarose concentrations (0.05 and 0.125%$_w$ - A1 and A2) was studied by collecting all the supernatants and replacing them with fresh PBS at each timepoint. Release quantification was performed, measuring protein content in the supernatant with the Bradford method, by spectrofluorimetry and by FACS (Becton Dickinson, FACSCalibur).

Protein Stability Analysis

NC and Ag (0.125%) NSPs loaded with BSA were treated with trypsin (25 μg/mL) for different times, and enzymatic digestion was ended, adding equal volumes of bleaching solution (20% acetonitrile-CH_3CN and 4% trifluoroacetic acid-TFA in water) at the different time points. The structural integrity of the BSA, released after 24 h from NC and Ag NSPs after the different trypsin treatments, was analyzed with sodium dodecyl sulfate polyacrylamide gel electrophoresis (SDS-page) using Criterion Tris–HCl Gel (BioRad) in non-reduced condition and high performance liquid chromatography (HPLC) (ELITE LaChrome, Itachi). Digestion products were also quantified analyzing SDS page silver stained bars with ImageJ.

Cell Culture and Confocal Microscopy

Human umbilical vein endothelial cells (HUVEC) were cultured in complete Dulbecco's modified eagle's medium (DMEM) at 37°C and in 5% CO_2 using two different systems: (a) four-chamber tissue culture-treated glass slides and (b) circular glass coverslip of 8 mm diameter placed in 12-well plates. 120,000 and 240,000 cells were seeded per chamber and well, respectively. Cells were allowed to settle for 2 h before adding NSPs. On the glass slide 600,000 NC or Ag NSPs loaded with BSA FITC-conjugated were added directly to the cells in each chamber and incubated for 24 and 48 h. In the multi-well plate 1,200,000 NC or Ag NSPs loaded with BSA FITC-conjugated were added in a transwell over the cells to each well, avoiding direct contact between cells and NSP.

Cellular internalization of NSPs and uptake of BSA were observed for both systems by confocal microscopy (Leica MD 6000) after 24 and 48 h incubation with Ag or NC particles. Cells were stained with fluorescent phalloidin (actin filaments) and DRAQ5 (nuclei) after fixation in 4% paraformaldehyde. Cellular uptake of BSA from 1 mg/mL BSA-FITC-conjugated solution prepared in DMEM was also evaluated. All images used for quantification were acquired by keeping the same acquisition setting (pinhole, gain, laser power, optical path, line average, zoom and image resolution) for the whole duration of the experiment. Numerical evaluation of the fluorescence was performed using the Nikon Elements software. The average fluorescence within the cytoplasm or the nuclei was measured in different representative fields of view (at least 5 cells per image per timepoint). Cellular uptake of BSA from protein dispersed in solution was not numerically quantified because by using the same confocal setting, most of the cells appeared supersaturated, thus not allowing a direct comparison between the two conditions.

Statistical Analysis

Reported data are the averages of at least three different measurements, and statistical significance ($p<0.05$) was evaluated with ANOVA (Origin), if not otherwise stated in the text.

RESULTS AND DISCUSSION

Characterization of Nanoporous Silicon Particles

NSPs used in this work were quasi-hemispherical shells of 3.2 μm diameter and 600 nm shell thickness (Fig. 1A and a) designed for drug delivery application (44). Pore size is 15 nm with 51% porosity as estimated from the desorption branch of nitrogen adsorption/desorption isotherms. APTES modification altered particles' surface charge (zeta potential from −23 mV to +1 mV) and allowed the loading of about 10 μg of BSA per million of NSP (7 μg). BSA is negatively charged and could not be loaded in oxidized particles (loaded particle zeta potential was −28 mV). This specific NSP structure, successfully employed in an *in vivo* delivery study (41), was chosen to investigate the NSP assembly and functions. It is worth noting that throughout the same fabrication process, NSPs of different size, shape, and porosity but with same chemical-physical properties, (29) could be used as substrate for the herein proposed agarose surface modification.

The agarose coating was developed and optimized to assure a protective function against harmful agents during long-term release. SEM images (Fig. 1B–E) indicated that the resulting agarose coating was uniform and density increased with agarose concentration. Agarose hydrogel matrix filled the pores and covered the particles' surface completely but did not alter appreciably the size and charge of the NSP (zeta potential was +2 and −30 mV for not-loaded and loaded NSPs, respectively).

Agarose coatings appeared to be uniform and smooth for all conditions considered. At the highest agarose concentrations (0.25 and 0.5%) hydrogel residues and particle aggregates appeared (see Supplementary Material). To assure stable uniform coating and good dispersion of the particles, 0.05 and 0.125% agarose concentrations (A1 and A2, respectively) were selected for further analysis, together with bare (not-coated (NC)) NSPs for comparison.

Degradation process of NC NSP as observed at SEM is shown in Fig. 2. SEM images show the progressive degradation of NSPs (into orthosilicic acid as assessed by ICP, data not shown (35,45,46) during degradation while their size slightly decreased. Degradation rate of exposed

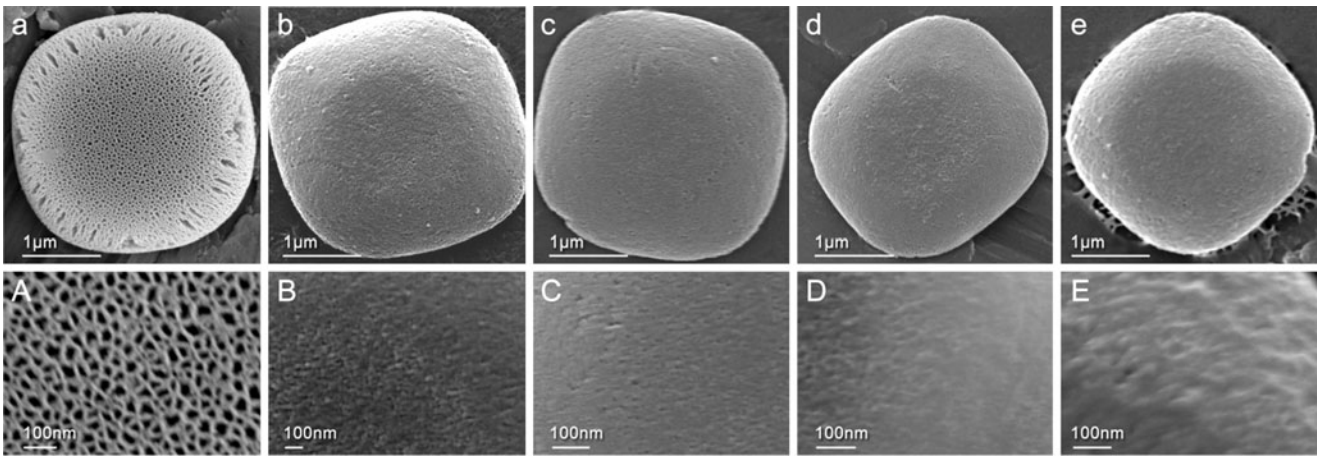

Fig. 1 Agarose modification of nanoporous silicon particles (NSP): NSP observed with SEM at low (lowercase letters) and high (uppercase letter) magnification: (**a** and **A**) bare NSP and (**b**, **c**, **d** and **e**) agarose coated NSP with different agarose concentration (0.05, 0.125, 0.25 and 0.5%, respectively).

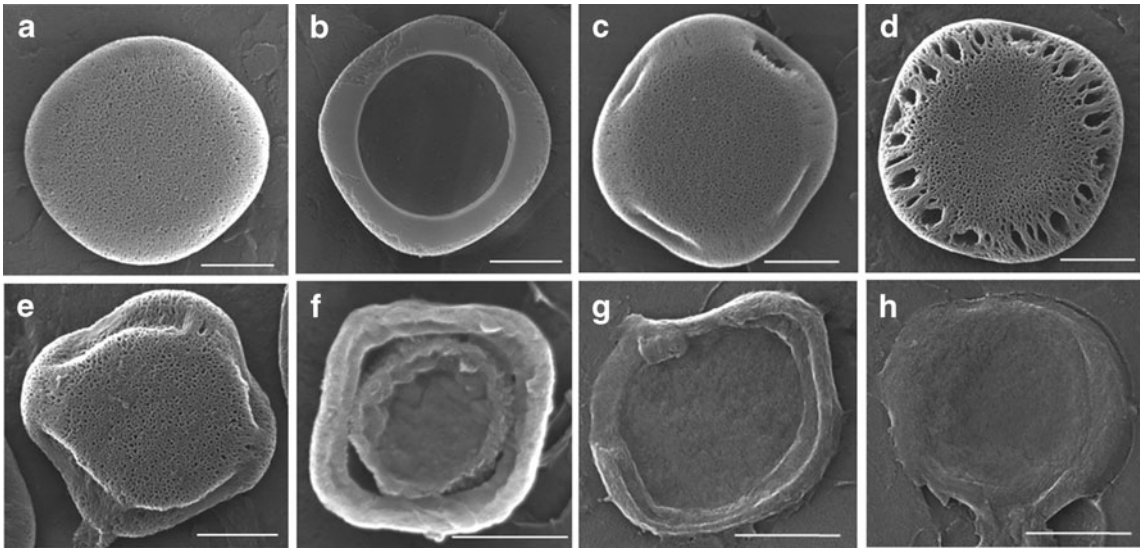

Fig. 2 Silicon particles (NSP) degradation: SEM observation at different times of NSP: bare NSP after (**a**) 2 h, (**b**) 4 h, (**c**) 8 h, (**d**) 12 h, (**e**) 1 day, (**f**) 2 days, (**g**) 3 days, and (**h**) 4 days of incubation with PBS. Scale bar is 1um.

silicon was uniform across the entire particle. As previously reported, we observed higher degradation in the outer rim because of the higher surface area and porosity of this structure (45).

NSP degradation over time was also monitored with flow cytometry (FACS) (Fig. 3a), quantifying NSP size variation through the change in the forward scattering intensity (Fig. 3b). Polystyrene beads of given size were used as calibration standards (Fig. 3c).

FACS data showed that NSP size reduced in three days from about 3 to almost 2 μm, as was observed also at the SEM. FACS analysis reveals no significant differences between NC and Ag NSP with either agarose concentrations (A1 and A2).

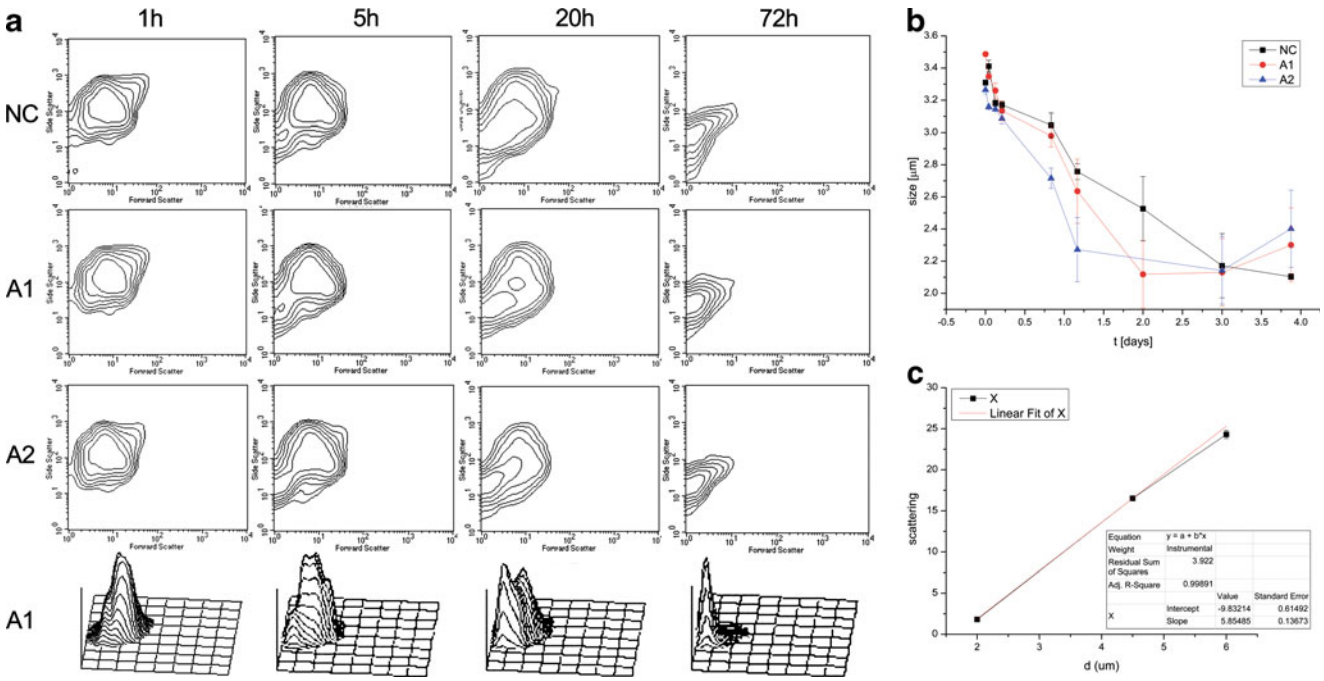

Fig. 3 Particles degradation as measured through FACS: (**a**) Forward and side scattering data analysis and (**b**) size measurements over time of bare (NC) and agarose-coated nanoporous silicon particles with two agarose concentrations (0.05 and 0.125%, A1 and A2, respectively).

Quantification of Protein Release

To assess protein release from Ag NSPs, fluorescent BSA was used as model. Loading and release of BSA from Ag NSPs with two agarose concentrations (A1 and A2) and NC NSPs were quantified by fluorescence spectroscopy. Loading efficiency was about 70% for both NC and Ag NSPs (Fig. 4a); hence, the agarose coating did not affect protein loading. FACS and spectrometric BSA release data are shown in Fig. 4b and c, respectively.

FACS results (Fig. 4b) showed that NSP fluorescence exponentially decreased ($y = A^{*}e^{\wedge B^{*}x} - R^2 > 0.91$) in three days. Moreover, there was no significant difference between NSP NC and Ag with both agarose concentrations. Spectrofluorimetry data (Fig. 4c) also showed that all the loaded protein was released with a logarithmic profile ($y = A^{*}\ln(x) + B - R^2 > 0.98$) within three days for NSP NC and Ag with both agarose concentrations. FACS and spectrofluorimetry data agreed showing that while the BSA was released from NSPs, the particles' fluorescence decreased accordingly (see Supplementary Material for fitting curves and parameters); after three days almost all BSA was released (~90%) and NSPs were almost not fluorescent anymore (~5%). Protein release study results indicated that agarose coating does not affect protein release from NSPs.

Released Protein Integrity Analysis

To assess the protection of protein integrity provided by agarose coating, BSA-loaded NSPs were treated with trypsin for 10, 30, 60 and 120 min, and released BSA solution analyzed with SDS page. Resulting gel for NC and Ag (composition A2) NSPs is shown in Fig. 5.

The gel analysis showed several protein fragments, digestion products, together with BSA and trypsin (when added), and no aggregates (see Supplementary Material). The concentration and number of fragments appeared higher in the solutions released from the NC NSPs. Moreover, the presence of protein fragments increased with trypsin treatment time, while trypsin and BSA amounts were about the same in all the samples.

To better quantify protein, enzyme, and digestion products the SDS result was also analyzed with ImageJ (see Supplementary Material) and the three most abundant digestion products plotted as function of trypsin treatment duration (Fig. 5). The quantitative analysis showed that solution recovered from NC NSP samples contained a higher concentration of digestion products' than the one recovered from Ag NSPs for all treatment conditions. The samples not treated with trypsin showed no difference between NC and Ag NSPs. The amount of BSA and trypsin was the same in all treated samples. The amount of fragments increased with trypsin treatment time for the NC NSP samples but was almost constant in the Ag NSPs.

HPLC analysis performed on BSA solution recovered after 24 h from NSPs not treated and treated with trypsin for 15 min, 2 h, 4 h, 8 h and 18 h is shown in Fig. 6. Graphs show an increase of digestion products, concentration and number with duration of trypsin treatment. There were more digestion products in the solution released by NC particles, especially for longer trypsin treatment time, as evidenced especially for the three species indicated by arrows. These results are in agreement with the SDS-page analysis and confirm the protective function of the agarose coating from enzymatic digestion.

Cellular Internalization of NSP and Uptake of Protein

Cellular uptake of protein was studied using fluorescent BSA and evaluating the fluorescence within HUVEC by

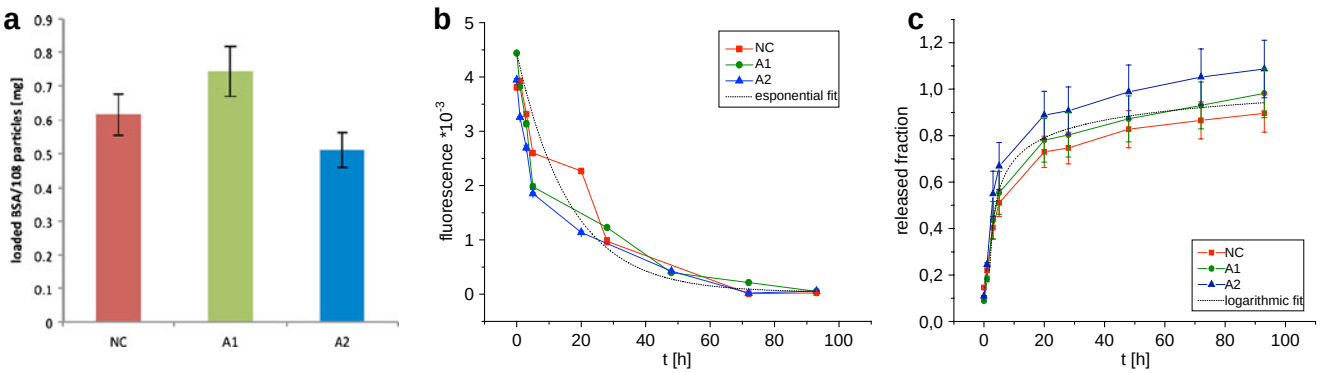

Fig. 4 Protein load and release: (**a**) Amount of BSA loaded in bare (NC) and agarose coated particles with two agarose concentrations 0.125 and 0.05% (A1 and A2, respectively); (**b**) fluorescence of agarose coated (A1 and A2) and NC nanoporous silicon particles (NSP), as measured at FACS, and (**c**) BSA released from agarose coated (A1 and A2) and NC NSP as measured with spectrofluorimetry.

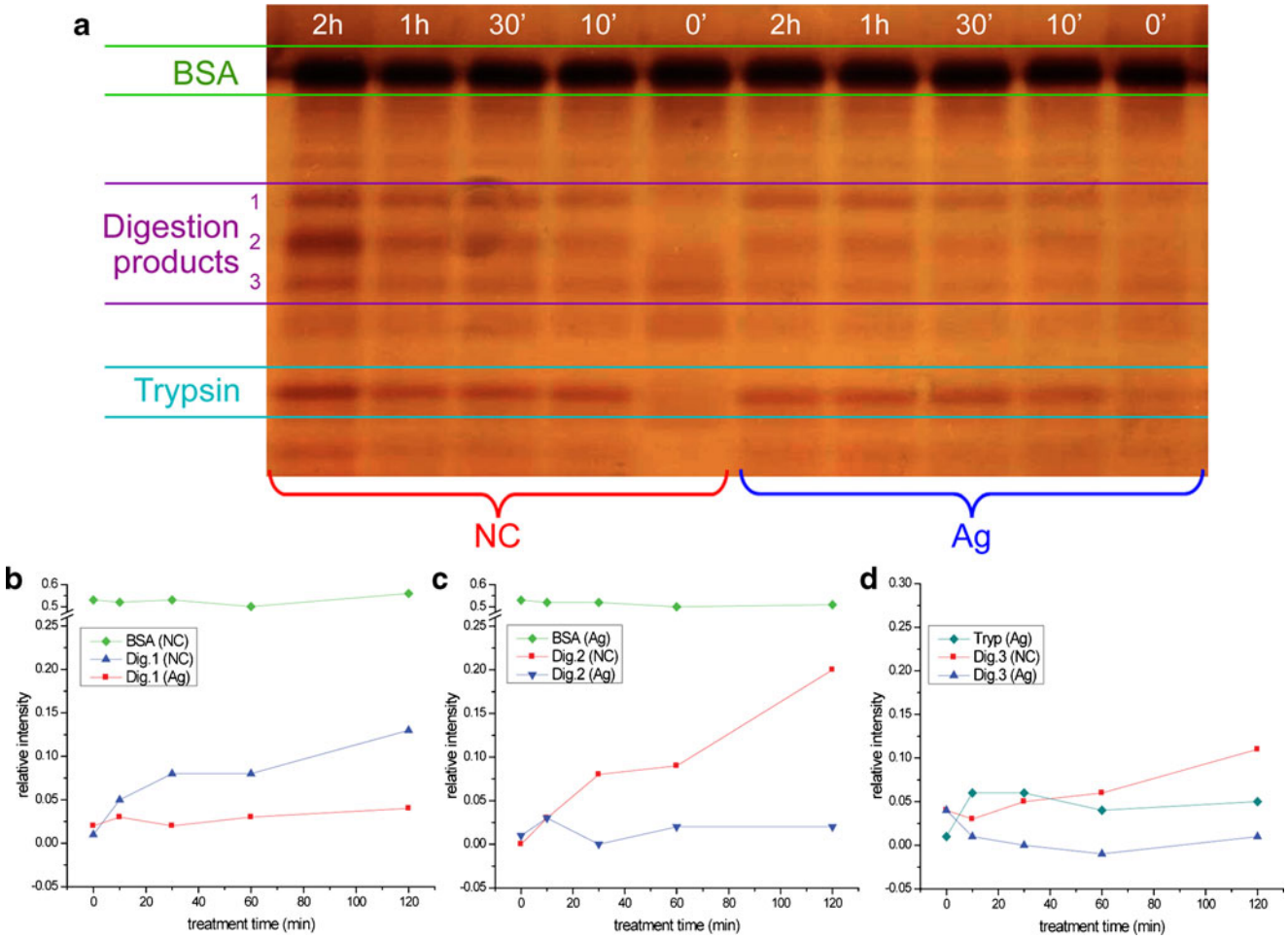

Fig. 5 Gel electrophoresis: (**a**) SDS-page of protein solution released after 24 h from bare (NC) and agarose-coated (Ag) nanoporous silicon particles treated for different times with trypsin (treatment duration in minutes, printed in white on each column). 1, 2 and 3 indicate the most abundant digestion products. (**b**, **c**, **d**) SDS-page relative intensity quantification with ImageJ of trypsin (Tryp), BSA and the three most abundant digestion products (Dig.1, 2 and 3) detected in the protein solution released after 24 h from bare (NC) and agarose-coated (Ag composition 0.125%) silicon particles after different trypsin treatment duration.

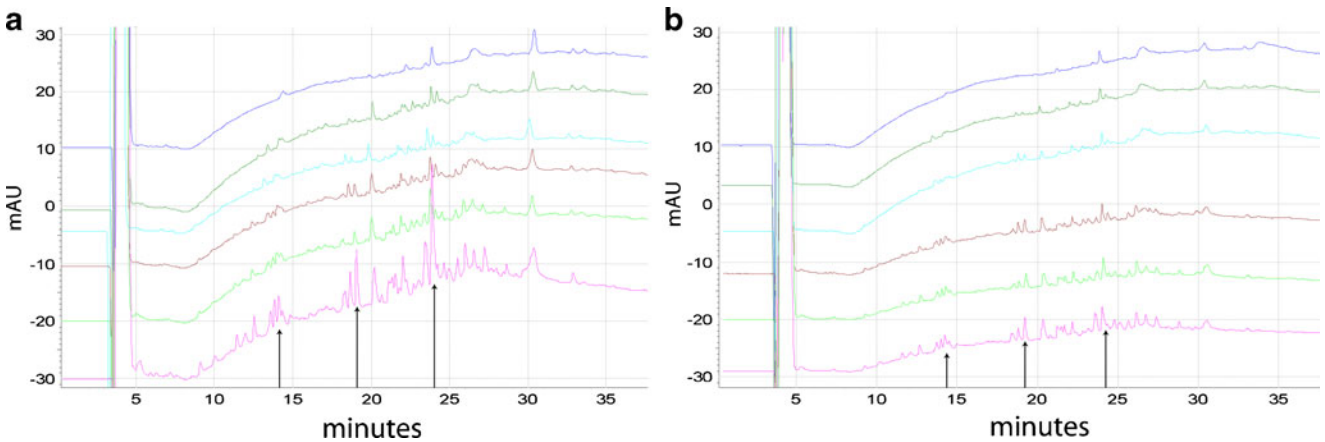

Fig. 6 Released protein solution chromatography (HPLC): HPLC analysis of BSA solution released after 24 h by (**a**) NC and (**b**) Ag particles not treated (*blue*) and treated with trypsin 15 min, 2, 4, 8 and 18 h (*green*, *light blue*, *brown*, *light green* and *pink* respectively). Arrows point to three digestion products the amount of which increases with trypsin treatment time.

confocal microscope imaging after 24 and 48 h. Particle internalization and BSA uptake after 48 h of incubation with NC and Ag (composition A2) NSPs added into the media with the cells or in a transwell on top of them are shown in Fig. 7. After 48 h of incubation with cells, both NC and Ag NSPs were completely internalized, and BSA was released within the cells. Confocal microscopy showed that the internalization process was not affected by the agarose coating, and NSPs accumulated in the lysosomes in less than 1 h, as previously reported (47).

NSP internalization was inhibited using the transwells, and BSA was first released in the media and then incorporated into the cells. Images show that uptake of BSA released from NSPs in the transwell or from BSA solution was not uniform within the cells, and the protein probably accumulated within the lysosomes. The fluorescence within the cells receiving BSA from the transwell was comparable with that of the cells that internalized NSPs. The cellular uptake of BSA from protein dispersed in solution (1 mg/mL) appears higher than the one achieved by NSP release (to avoid pixel oversaturation, different confocal settings were used to acquire Fig. 7f). This can be attributed to less BSA being released from NSPs resulting in a lower overall BSA concentration in the media.

A difference in the cellular uptake of BSA between internalized Ag and not-coated particles was observed. We hypothesized that the agarose coating was able to induce a change of pH within the lysosomes and influence the cellular uptake. To assess if the agarose coating matrix would affect the pH within the lysosomes, different volumes of pH 5 solution and agarose coating solution were mixed at room temperature, and the change of pH was measured (Fig. 8).

pH increased from 5 to 6 or more, depending on the ratio of agarose coating solution (AG), while no change of pH was observed if agarose was prepared with DI water instead of PBS. This experiment revealed that the agarose solution used to coat the particles had a buffering capacity which could have been instrumental for the local modification of the pH in the small acidic lysosomal environments.

The progression over time of the uptake process relative to HUVEC incubated with NC and Ag NSPs is shown in Fig. 9. After 24 h of NSP incubation, cellular uptake of BSA was visible but still not evident especially for NC NSPs. BSA accumulated in the cells where the NSPs, both NC and Ag particles, were internalized. The protein escaping from the lysosomes was uniformly distributed throughout the nuclei and the cytoplasm of the cells. We hypothesize that the agarose coating affected lysosome pH once NSPs were internalized and hence facilitated protein escape.

To better quantify the BSA uptake within the cells, the average green fluorescence intensity of confocal images within the cytoplasm and the nucleus of the cells was

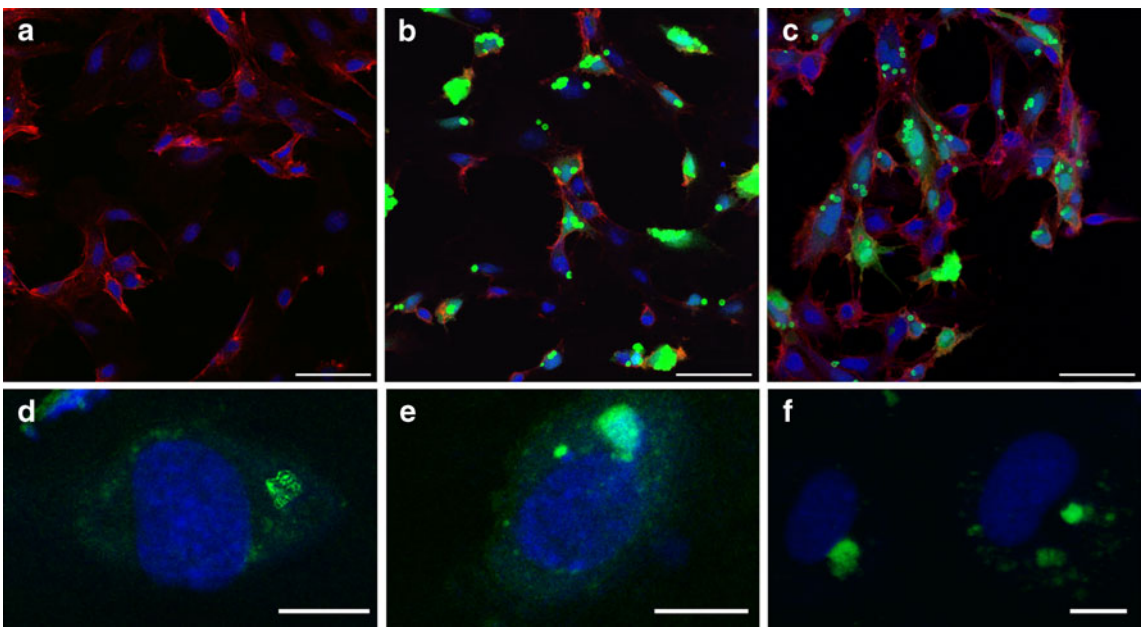

Fig. 7 *In vitro* confocal study of cellular internalization of silicon particles (NSP) and protein uptake: cells (HUVEC) incubated for 48 h (**a**–control) without NSP; (**b**) with BSA-loaded NSP added into the media; (**c**) with agarose-coated BSA loaded NSEs added into the media; with (**d**) NC and (**e**) Ag BSA-loaded NSP placed in a transwell on top of the cells, or in (**f**) BSA solution. White scale bar is 50 μm in **a**, **b** and **c**, and 10 μm in **d**, **e** and **f**.

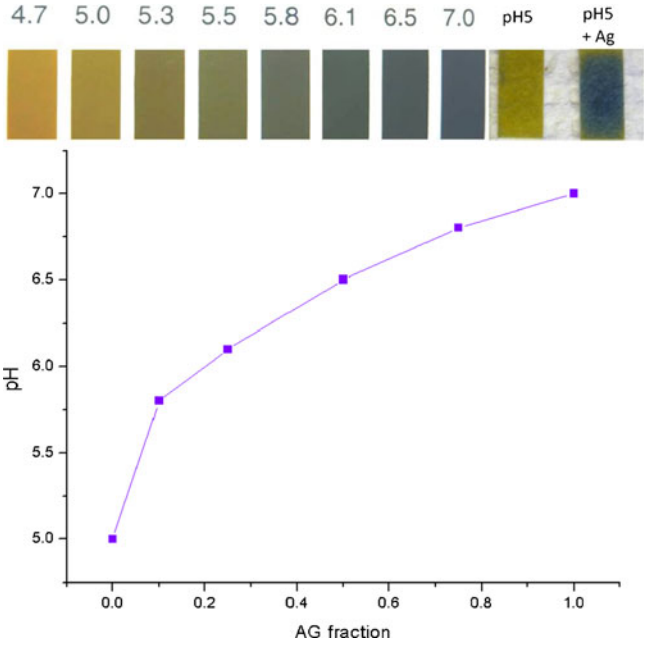

Fig. 8 pH measurement of acid solution change due to agarose coating solution.

quantified with Elements (Nikon) and correlated with the number of NSPs internalized in each cell (Fig. 9). Data showed a higher uptake of BSA within cells incubated with Ag NSPs than with NC NSPs. Uptake of the protein was also proportional to the number of particles internalized. Uptake of BSA released from Ag NSPs increased more rapidly with the number of internalized NSPs than from NC NSPs. Additionally, protein accumulated within the nuclei more than within cytoplasm.

These data suggested that agarose coating increases cellular uptake of the protein and avoids extended entrapment in the lysosomes.

CONCLUSION

In this work we successfully modified with hydrogel NSPs, designed and fabricated for drug delivery application, to improve their efficacy for intracellular protein release. We verified that the agarose coating protects the payload from enzymatic digestion, while it does not affect its release from the NSPs. We also showed that the hydrogel coating increases cellular uptake and influences intracellular trafficking of the protein in comparison with what was observed from proteins dispersed in solution. Furthermore, the agarose coating is able to improve intracellular protein delivery and increases the accumulation of the protein within the nuclei. Thus, the agarose coating of NSPs may extend the use of pSi as versatile delivery system for enzymes, vaccine antigens, gene therapy, and other protein therapeutics. Additionally, it may act effectively in combination with other controlled release systems (e.g. PLGA encapsulation) to preserve protein stability during controlled drug delivery formulation and long-term release.

ACKNOWLEDGMENTS

Special thanks to our silicon fabrication team and the Microelectronics Research Center at the University of Texas at Austin. We thank M. Landry for the graphical support and I. Yazdi for the silicon particles modification

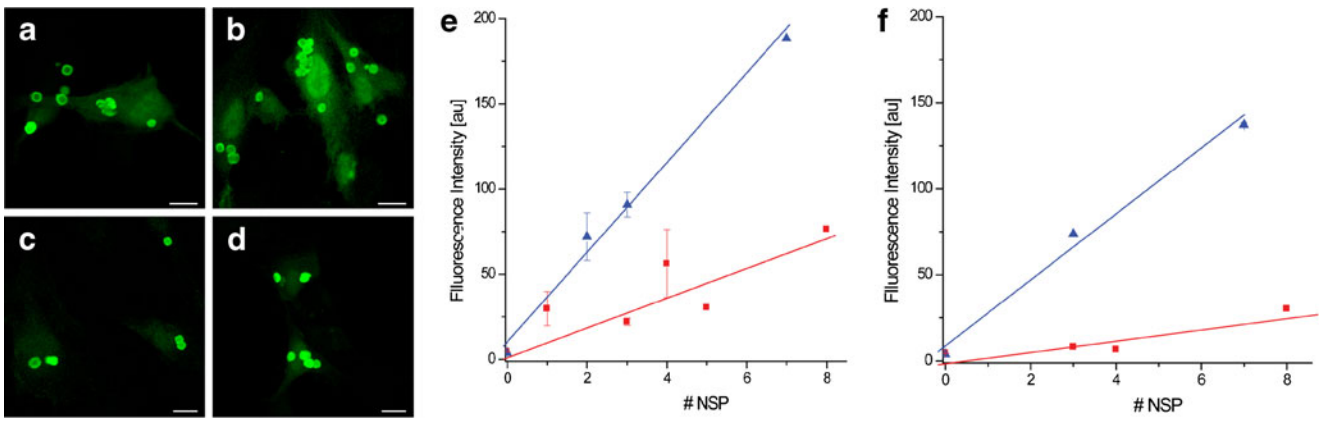

Fig. 9 Confocal study of cellular uptake of protein from internalized particles (NSP): HUVEC incubated for (**a**, **c**) 24 h and (**b**, **d**) 48 h with (**a**, **b**) FITC-BSA-loaded agarose-coated NSP, (**c**, **d**) FITC-BSA-loaded not coated NSP. Scale bar is 10 μm. (**e**, **f**) Quantification of uptake of BSA within the cells: fluorescence intensity within (**e**) the nucleus and (**b**) the cytoplasm of the cells quantified with NIS-Elements. Red square and blue triangle refer to NC and Ag NSP, respectively.

and characterization. This study was supported by the following funds: DoD W911NF-09-1-0044 and State of Texas Governor's Emerging Technology Fund.

REFERENCES

1. Leader B, Baca QJ, Golan DE. Protein therapeutics: a summary and pharmacological classification. Nat Rev Drug Discov. 2008;7:21–39.
2. Murphyand WJ, Longo DL. Growth hormone as an immunomodulating therapeutic agent. Immunol Today. 2000;21:211–3.
3. Chen DJ, Osterrieder N, Metzger SM, Buckles E, Doody AM, DeLisa MP, *et al.* Delivery of foreign antigens by engineered outer membrane vesicle vaccines. Proc Natl Acad Sci. 107:3099–3104.
4. Rosado JL, Solomons NW, Lisker R, Bourges H. Enzyme replacement therapy for primary adult lactase deficiency. Effective reduction of lactose malabsorption and milk intolerance by direct addition of [beta]-galactosidase to milk at mealtime. Gastroenterology. 1984;87:1072–82.
5. Haase M. Human recombinant factor IX: safety and efficacy studies in hemophilia B patients previously treated with plasma-derived factor IX concentrates. Blood. 2002;100:4242.
6. Mease PJ. Etanercept in the treatment of psoriatic arthritis and psoriasis: a randomised trial. Lancet. 2000;356:385–90.
7. Gorman JD, Sack KE, Davis JC. Treatment of ankylosing spondylitis by inhibition of tumor necrosis factor [alpha]. N Engl J Med. 2002;346:1349–56.
8. Szmuness W. Hepatitis B vaccine: demonstration of efficacy in a controlled clinical trial in a high-risk population in the United States. N Engl J Med. 1980;303:833–41.
9. Shi L. Gardasil: prophylactic human papillomavirus vaccine development [mdash] from bench top to bed-side. Clin Pharm Ther. 2007;81:259–64.
10. Sodee DB. Multicenter ProstaScint imaging findings in 2154 patients with prostate cancer. Urology. 2000;56:988–93.
11. Taillefer R, Edell S, Innes G, Lister-James J. Acute thromboscintigraphy with Tc-99 m-apcitide: results of the phase 3 multicenter clinical trial comparing Tc-99 m-apcitide scintigraphy with contrast venography for imaging acute DVT. J Nucl Med. 2000;41:1214–23.
12. Meier CA. Diagnostic use of recombinant human thyrotropin in patients with thyroid carcinoma (phase I/II study). J Clin Endocrinol Metab. 1994;78:188–96.
13. VeÌgvaÌriand A, Marko-Varga G. Clinical Protein Science and Bioanalytical Mass Spectrometry with an Emphasis on Lung Cancer. Chem Rev. 2010;110:3278–98.
14. McVey D, Hamilton MM, Hsu C, King CR, Brough DE, Wei LL. Repeat Administration of Proteins to the Eye With a Single Intraocular Injection of an Adenovirus Vector. Mol Ther. 2008;16:1444–9.
15. Mahmoodand I, Green MD. Pharmacokinetic and pharmacodynamic considerations in the development of therapeutic proteins. Clin Pharmacokinet. 2005;44:331–47.
16. Putneyand SD, Burke PA. Improving protein therapeutics with sustained-release formulations. Nat Biotech. 1998;16:153–7.
17. Fu K, Klibanov AM, Langer R. Protein stability in controlled-release systems. Nat Biotech. 2000;18:24–5.
18. Tayaliaand P, Mooney DJ. Controlled growth factor delivery for tissue engineering. Adv Mater. 2009;21:3269–85.
19. Edelman ER, Nugent MA, Karnovsky MJ. Perivascular and intravenous administration of basic fibroblast growth factor: vascular and solid organ deposition. Proc Natl Acad Sci USA. 1993;90:1513–7.
20. Lazarous DF, Shou M, Scheinowitz M, Hodge E, Thirumurti V, Kitsiou AN, *et al.* Comparative effects of basic fibroblast growth factor and vascular endothelial growth factor on coronary collateral development and the arterial response to injury. Circulation. 1996;94:1074–82.
21. Wang J, Chua KM, Wang C-H. Stabilization and encapsulation of human immunoglobulin G into biodegradable microspheres. J Colloid Interface Sci. 2004;271:92–101.
22. van de Weert M, Hennink WE, Jiskoot W. Protein Instability in Poly(Lactic-co-Glycolic Acid) microparticles. Pharm Res. 2000;17:1159–67.
23. Sah H. Protein instability toward organic solvent/water emulsification: implications for protein microencapsulation into microspheres. PDA J Pharm Sci Technol. 1999;53:3–10.
24. Cleland JL, Mac A, Boyd B, Yang J, Duenas ET, Yeung D, *et al.* The stability of recombinant human growth hormone in poly(lactic-co-glycolic acid) (PLGA) microspheres. Pharm Res. 1997;14:420–5.
25. Canham LT. Bioactive silicon structure fabrication through nanoetching techniques. Advanced Materials. 1995; 7.
26. Voelcker NH, Khung Y-L, Low SP, Clements LR, Williams KA. Porous Silicon Science and Technology Conference, Valencia, 2010.
27. Herino R. In: Canham LT, editor. The properties of porous silicon. London: INSPEC-IEE; 1997.
28. Salonen J, Kaukonen AM, Hirvonen J, Lehto VP. Mesoporous silicon in drug delivery applications. J Pharm Sci. 2008;97:632–53.
29. Chiappini C, Tasciotti E, Fakhoury JR, Fine D, Pullan L, Wang Y-C, *et al.* Tailored porous silicon microparticles: fabrication and properties. Chemphyschem. 2010;11:1029–35.
30. Cunin F, Schmedake TA, Link JR, Li YY, Koh J, Bhatia SN, *et al.* Biomolecular screening with encoded porous-silicon photonic crystals. Nat Mater. 2002;1:39–41.
31. Linsmeier J, Wüst K, Schenk H, Hilpert U, Ossau W, Fricke J, *et al.* Chemical surface modification of porous silicon using tetraethoxysilane. Thin Solid Films. 1997;297:26–30.
32. Gurtner C, Wun AW, Sailor MJ. Surface modification of porous silicon by electrochemical reduction of organo halides. Angew Chem Int Ed. 1999;38:1966–8.
33. Salonen J, Laitinen L, Kaukonen AM, Tuura J, Björkqvist M, Heikkilä T, *et al.* Mesoporous silicon microparticles for oral drug delivery: Loading and release of five model drugs. J Control Release. 2005;108:362–74.
34. Prestidge CA, Barnes TJ, Lau CH, Barnett C, Loni A, Canham L. Mesoporous silicon: a platform for the delivery of therapeutics. Expert Opin Drug Deliv. 2007;4:101–10.
35. Tasciotti E, Liu XW, Bhavane R, Plant K, Leonard AD, Price BK, *et al.* Mesoporous silicon particles as a multistage delivery system for imaging and therapeutic applications. Nat Nanotechnol. 2008;3:151–7.
36. Prestidge CA, Barnes TJ, Mierczynska-Vasilev A, Kempson I, Peddie F, Barnett C. Peptide and protein loading into porous silicon wafers. Phys Status Solidi A. 2008;205:311–5.
37. Prestidge CA, Barnes TJ, Mierczynska-Vasilev A, Skinner W, Peddie F, Barnett C. Loading and release of a model protein from porous silicon powders. Phys Status Solidi A. 2007;204:3361–6.
38. Serda RE, Godin B, Blanco E, Chiappini C, Ferrari M. Multi-stage delivery nano-particle systems for therapeutic applications. Biochimica et Biophysica Acta (BBA)—General Subjects. In Press, Corrected Proof:in press (2010).
39. Kilpeläinen M, Riikonen J, Vlasova MA, Huotari A, Lehto VP, Salonen J, *et al. In vivo* delivery of a peptide, ghrelin antagonist, with mesoporous silicon microparticles. J Control Release. 2009;137:166–70.
40. Anglin EJ, Schwartz MP, Ng VP, Perelman LA, Sailor MJ. Engineering the chemistry and nanostructure of porous silicon

fabry-pérot films for loading and release of a steroid. Langmuir. 2004;20:11264–9.
41. Tanaka T, Mangala LS, Vivas-Mejia PE, Nieves-Alicea R, Mann AP, Mora E, *et al.* Sustained small interfering RNA delivery by mesoporous silicon particles. Cancer Res. 2010;70:3687–96.
42. Tanaka T, Godin B, Bhavane R, Nieves-Alicea R, Gu J, Liu X, *et al. In vivo* evaluation of safety of nanoporous silicon carriers following single and multiple dose intravenous administrations in mice. Int J Pharm. 2010;402:190–7.
43. Decuzzi P, Godin B, Tanaka T, Lee SY, Chiappini C, Liu X, *et al.* Size and shape effects in the biodistribution of intravascularly injected particles. J Control Release. 2010;141:320–7.
44. Ferrari M. Nanogeometry Beyond drug delivery Nat Nano. 2008;3:131–2.
45. Godin B, Gu J, Serda RE, Bhavane R, Tasciotti E, Chiappini C, *et al.* Tailoring the degradation kinetics of mesoporous silicon structures through PEGylation. J Biomed Mater Res A. 2010;94A:1236–43.
46. Serda RE, Mack A, Pulikkathara M, Zaske AM, Chiappini C, Fakhoury JR, *et al.* Cellular association and assembly of a multistage delivery system. Small. 2010;6:1329–40.
47. Ferrati S, Mack A, Chiappini C, Liu X, Bean AJ, Ferrari M, *et al.* Intracellular trafficking of silicon particles and logic-embedded vectors. Nanoscale. 2010;2:1512–20.